LA-UR-99-2648

Title: **Model Inversion Using Bayesian Inference And Genetic Algorithms Part IV: Micromechanical Modeling of Powder Consolidation and Sintering**

Author(s): Brian J. Reardon, MST-6

Submitted to:

http://lib-www.lanl.gov/la-pubs/00326797.pdf

Los Alamos
NATIONAL LABORATORY

Model Inversion Using Bayesian Inference And Genetic Algorithms Part IV: Micromechanical Modeling of Powder Consolidation and Sintering

Brian J. Reardon, MST-6, Los Alamos National Laboratory, Los Alamos, NM 87545

Abstract

The application of Bayesian analysis to genetic algorithm (GA) optimization of micromechanical powder densification models rectifies a number of deficiencies in the overall GA technique. Firstly, the stochastic noise of the GA is suppressed and thus a realistic assessment of model parameter sensitivities and correlations are now available using a GA. Secondly, a suitable stopping criteria for the GA is defined by when the sum of the eigenvalues obtained from the principle component analysis of the *a posteriori* covariance matrix reaches a limiting value. Lastly, the generation of the posterior probability density allows a distribution of optimal model parameter vectors to be applied to the physics of the forward problem. The distribution of the resulting outcomes is then used as a guide in experimental design.

1.0 Introduction

1.1 Inverse and Ill Posed Problems in Materials Science and Engineering

There is an ever increasing need in materials science and engineering to fit the parameters of models, which are to be used in a predictive capacity, using underdetermined experimental data sets. Model inversion of this type falls under the general category of inverse and ill – posed problems and can often be cast into the framework of Bayesian statistics (Tarantola, 1987). Such problems include state function determination, chemical potential determination from limited phase diagram data containing a high degree of uncertainty, and mechanical threshold strength determination from mechanical tests also with a high degree of uncertainty. In all of these examples, model parameters must be optimized using limited and uncertain data sets that leave the inversion underdetermined. Likewise, if the models are to be used in a predictive capacity, there is a need to be able to quantify the expected deviation of the model from reality.

This report shows how a fuzzy logic based multi-objective genetic algorithm (GA) (Reardon 1999) can be used as a Bayesian Inference Engine (BIE) to evolve a posterior probability density (PPD) of the model parameter vector space:

$$M_i = \{m_1, m_2, m_3, \ldots, m_N\}^T. \qquad \text{Eq. 1}$$

M_I is a particular model to be tested, m_J is one of the N parameters used in the model, and T signifies the transpose of the vector. The GA evolves a set or population of M_I's which effectively defines the PPD. Once the PPD has been sufficiently determined by the GA, parameter vectors are selected and used in the physics of the forward problem to evaluate the predictive capacity of the model.

The problem to be addressed through the use of GA's and Bayesian inference lies in the general realm of the micromechanical modeling of powder consolidation and sintering. Ashby's micromechanical model (Reardon, 1998b) has 19 parameters that

must be optimized so that the calculated densities match experimental densities for given processing conditions. The experimental data to be used here is for hot pressed copper powder data (Wadley *et al.* 1991) as well as warm isostatically pressed beryllium powder data (Roberts' 1983). The micromechanical model as well as the data used for the optimization has been discussed extensively in previous reports (Reardon, 1998a, 1998b) and thus will not be reviewed here.

1.2 Bayesian Statistics in Model Inversion

Consider a model parameter vector such as the one defined for the micromechanical powder consolidation problem in which 19 variables must be optimized:

$$M=\{m_1, m_2,\ldots m_{19}\}^T \qquad \text{Eq. 2}$$

and also consider a data vector defined as:

$$D=\{\rho_1, \rho_2,\ldots \rho_N\}^T. \qquad \text{Eq. 3}$$

Where N is the number of data points and can be very large. The goal of Bayesian analysis is to come up with a way of accepting or rejecting a particular model (M) or hypothesis given an experimental data set (D) and prior knowledge about the problem. Thus, in Bayesian statistics, the model or hypothesis is assigned a probability of acceptance and the total probability distribution function (PDF) of a series of models being tested makes up what is commonly called the posterior probability density (PPD). This goal is achievable through the central tenant of Bayesian statistics, Bayes' Theorem:

$$\sigma(M \mid D) = \frac{P(M,D)}{P(D)} = \frac{P(D \mid M)P(M)}{\int P(D,M)dM} \qquad \text{Eq. 4}$$

which is essentially the definition of conditional probability. This rule was first proposed by Rev. Thomas Bayes and published posthumously in 1763 but has been ignored up until the last 20 years due to the computational difficulties in evaluating the probability integrals (Bayes, 1763). This theorem says that the conditional probability of a model being correct given a set of data is a ratio of the PDF of M and D to the PDF of D alone. In Bayes' Theorem, the term P(D | M) is not a PDF but a likelihood function. Thus, while the individual components of P(D | M) are probabilities, the function itself does not integrate to 1.0.

Bayes' rule as written above differs considerably from classical frequentist statistics because of the dependence of the PPD on the prior PDF, P(M). P(M) often contains subjective information about the problem that the experimentalist has *a priori*. Another major departure from frequentist statistics is the way the PPD is updated as new experimental data becomes available. The frequentist view point is that P(D) should be considered an unchanging distribution and also that it is inappropriate to try to assign a probability of correctness to a hypothesis.

Consequently, Bayes' Rule provides the scientist with a tool that classical statistics is not capable or providing, namely, a mathematical formalization of the scientific method. When a phenomenon is observed, a hypothesis explaining the event is often created with the observer's own bias and experience in mind. This hypothesis is then tested against new experimental data and if the data supports the hypothesis then the belief in or probability of acceptance of the hypothesis increases. An excellent introduction to the Bayesian approach to hypothesis testing can be found in Chapter 4 of Antelman (1997).

The main difficulty in using Bayes' rule, lays in the evaluation of the denominator:

$$P(D) = \int P(D,M)dM, \qquad \text{Eq. 5}$$

where the integral is formally carried over the entire N-dimensional (in this problem, N = 19) model parameter space. The accurate and fast approximation of the integration of

an N-dimensional, discontinuous PDF is the topic of many papers. Duijndam (1988a, 1988b) discussed the use of Bayes' Rule in model inversion and accomplished the above integration by assuming the PPD had a Gaussian shape then optimized the Gaussian parameters using least squares. Unfortunately, most PPD's are not Gaussian in nature and thus other techniques were needed. These techniques include Monte Carlo integration, Gibb's Sampling, and genetic algorithms (Sen and Stoffa ,1992, 1996; Sen et al., 1993; Mallick, 1995; Gerstoft, 1998).

The PPD is a difficult function to visualize due to its multidimensionality and its change with every new experimental data point. However, once the PPD is derived, regardless of the method, a number of important parameters describing it can be easily calculated.

The mean model can be calculated:

$$\langle M \rangle = \int M \sigma(M \mid D) dM. \qquad \text{Eq. 6}$$

Likewise, the *a posteriori* model covariance matrix is given by:

$$C_M = \int (M - \langle M \rangle)(M - \langle M \rangle)^T \sigma(M \mid D) dM. \qquad \text{Eq. 7}$$

The covariance matrix provides a number of useful parameters. The standard deviation associated with the mean model is obtained through the square roots of the diagonal elements of C_M. Normalization of C_M through:

$$C_{ij} = \frac{C_{ij}}{\sqrt{C_{ii}}\sqrt{C_{jj}}} \qquad \text{Eq. 8}$$

produces the correlation matrix.

With C_M determined, a principle component analysis (PCA) will provide valuable insight on how well the GA is converging and what model parameters are most

significant or sensitive. In PCA the data of the C_M is transformed into a new set of axes of the same number which are orthogonal to each other and are ordered based on the variance associated with that axis. The principle components of C_M can be obtain by computing its set of eigenvalues (Λ) and corresponding orthogonal eigenvectors (U) such that:

$$C_M = U\Lambda U^T \qquad \text{Eq. 9}$$

is satisfied. In a d-dimensional variable space there are d eigenvalues or principle components. However, many principle components may have small variances and thus the intrinsic dimensionality of C_M is k where $k<d$.

In the context of a PPD evolved by a GA, PCA is a powerful tool that assists in overcoming many deficiencies in GA's. First, as the population evolves, the sum of the eigenvalues of C_M approaches a limit. When the rate of convergence reaches an acceptable minimum the GA can be stopped. Second, the largest eigenvalues and their corresponding eigenvectors indicate the most significant variables or groups of variables in the model given the available data. Thus, PCA acts as a form of sensitivity analysis for the variables in the model.

Once a PPD has been determined to be reliable based on the stabilization of the eigenvalues, an optimum model can be selected.

1.3 Genetic Algorithms in Model Inversion and Parameter Optimization

A detailed account of how a GA operates has been provided elsewhere (Reardon 1998a, 1999). In short, a GA randomly generates a set or population of parameter vectors M_i's where i = 1 to N and N is the population size. This initial selection, which occurs within parameter ranges set by the user, constitutes the *a priori* information used in Bayes' Theorem. From this set, parameter vectors that satisfactorily solve the optimization problem are selected. The selected members, which are each defined by a haploid binary string, exchange string components and thus create new members. The bits of the new member's strings are then randomly flipped with a small degree of

probability from 1 to 0 or vice versa. The final members are then inserted into the next generation. Once the next generation is filled the GA starts over with selection, crossover and mutation.

Since the GA acts as a BIE in that it uses Bayes' Theorem to select members in the population for crossover, the output of the GA is a PPD. The generation of a PPD now allows for many of the tools available in Bayesian statistics to be used in the analysis of the output of the GA. Namely from the PPD we can derive <M> and C_M. The beauty of this approach is that the PPD can be generated at virtually no extra cost. Following the method outlined by Sen and Stoffa (1992), a 2-D array of M X B is reserved where M is the number of parameters and B is the number of values each variable can take (i.e. the number of bins). For each model at each generation an unnormalized PPD, $\sigma(M)$, is computed and stored in the proper position in the bin array for each model parameter comprising each model. At the end of the GA run the model parameter PPD values are normalized. Also in a vector of length M, each component of M $\sigma(M)$ is stored and summed with the correspond values from the other models. This vector provides <M>. C_M is determined by summing up $MM^T \sigma(M)$ in a square array of MM for each model and at the end of the run subtracting $<M><M>^T$. The FORTRAN 90 code used to evaluate these quantities was presented previously (Reardon 1999).

Once the PPD, <M>, and C_M have been sufficiently determined, the GA can be stopped and optimal model parameter vectors can be selected and used in the physics of the forward problem for conditions that have not been experimentally tested.

2.0 Optimizing the parameters of the Ashby Micromechanical Model for Beryllium Powder

Previous work published regarding the use of GA's to optimize parameters of Ashby's micromechanical powder densification model (Reardon 1998b, 1998c) presented graphs such as those of Figure 1. Figure 1 shows the average objective value for the entire population as a function of generation along with the standard deviation of the average. Since each objective is defined to be a minimization of the difference between the experiment and theory, one would expect the average for the

population to go to zero. Similar graphs can be made for the actual variables being optimized. Such graphs are shown in Figures 2a and 2b for the yield stress and surface energy of beryllium powder. Examination of figures 2a and 2b indicates that some variables (such as yield stress) converge quite rapidly whereas other variables do not. This fact would indicate that for the given set of data, yield stress is a very important or sensitive parameter. However, such ratiocination is problematic for two reasons. First, there is no way of filtering out the inherent stochasticity of the GA. Consequently, it is impossible to determine how much of the standard deviation of the average is due to noise and how much is due to a legitimate variation that exists due to the model being underdetermined. Second, inspection of graphs such as this provides no insight as to how the parameters may be correlated. A third problem with underdetermined model inversion is shown in figure 3. Figure 3. shows the result of a copper powder optimization (Reardon 1998c). In this work the GA optimized the Ashby model using the data of Wadley *et al*.(1991), then five optimal members were selected from the evolved population and implemented into the forward model under the original experimental processing conditions. The conditions here involved ramping the temperature and pressure up to 723K and 50MPa for 15000s and holding constant for another 15000s. As figure 3. shows all of the models reach approximately the same final end point but the path each took to get there is considerably different. This fact would then indicate that just because a model fits a particular data set, we can not necessarily use the model in any sort of predictive capacity.

A fourth problem deduced from figures 2a,b revolve around the issue of a finding a suitable stopping criteria for the GA. The yield stress data would indicate that the GA could be stopped at 30 generations whereas the surface energy data would indicate that more optimization is necessary. It will be shown here that the application of Bayes Theorem will help to resolve these problems.

The issue of suppressing the inherent noise of the GA so that a real signal can be obtained is shown in the marginal PPD plot for Beryllium yield stress in Figure 4a,b. Figure 4a shows the unnormalized beryllium yield stress PPD at generation 0 and figure

4b shows it at generation 80. As these graphs show, the calculation of the PPD suppresses the noise inherent within the GA and thus provides a clear signal for the parameter values.

The yield stress value of figure 4b is approximately 5 times higher than the currently accepted bulk value for beryllium. The reason the GA optimized the model to such a high yield stress is because of a faulty assumption built into the model about the geometry of a powder compact. The micromechanical model presented here assumes that the powder consists of a dense random packing of monosized spheres that are in point contact. However, the real beryllium powder consists of attrition milled platelets in face contact. Obviously, the yielding behavior of the two powders will be different and the GA optimizes the yield stress of the powder to account for this difference.

PCA of the C_m for the beryllium optimization problem resolves a number of other problems. Figure 5 shows the evolution of all 20 eigenvalues as a function of generation. The C_m is a 20 X 20 matrix corresponding to the 19 variables being optimized plus a dummy variable included in the optimization to ensure the proper performance of the GA. In PCA, the largest eigenvalues are the most significant and correspond to eigenvectors that indicate the most important or significant variables in the optimization. Thus the largest two eigenvalues have eigenvectors that are dominated by the yield stress and the power law creep reference stress. The next largest eigenvalue has a corresponding eigenvector dominated by the creep transition temperature, volume diffusion activation energy, and the power law creep reference stress. This data can be viewed in two ways. First, one can assume that given the processing conditions provided in the data all one has to do is test powder properties related to yield stress and powder law creep reference stress in order to ensure that the powder will behave properly. On the other hand, one can look at the variables that are deemed to be insignificant according to PCA and then collect data in the regimes believed to activate those mechanisms. In Table I, the most significant parameters for each eigenvector are in bold down to the eigenvector dominated by the random

variable. Model parameters less sensitive than the dummy variable correspond to mechanisms that are not active to any significant extent.

Another advantage of PCA lies in the fact that the sum of the eigenvalues approaches a limit as the GA evolves. As in the case of D-optimal design of experiments, when the sum reaches a limit, the optimization can be stopped.

The final point to be addressed in the beryllium powder optimization problem lies in the realm of experimental design. Since the GA provides a distribution of optimum models this distribution can be used to calculate the expected average relative density of the model along with its uncertainty. Figure 6 shows the expected average relative density for the unoptimized model distribution. As a function of temperature and pressure where the simulation incorporates a 1 hour ramp up, 1 hour hold, and 1 hour ramp down. This graph essentially depicts the *a priori* model distribution (P(M)) in Bayes' theorem. Figure 7 shows the standard deviation of the average relative density shown in figure 6. Clearly the robustness of the model would benefit from data collected within the vicinity of 1100K and 0MPa. In other words, a sintering experiment is clearly needed to make this model more robust. After the model was optimized using warm isopressed data (Roberts, 1983) a similar average expected densification plot can be generated. This is shown in figure 8. The uncertainty of figure 8 is shown in figure 9. From the comparison of figures 7 and 9 one can see how the maximum uncertainty of the model dropped from 0.146 to 0.139. While this drop is not impressive, there is a significant change in the uncertainty landscape of the two plots. Inspection of Figure 9 again shows the need for sintering data in the vicinity of 1100K.

3.0 Optimizing the parameters of the Ashby Micromechanical Model for Copper Powder

As similar analysis of Wadley *et al.*'s (1991) copper powder data was also conducted. Figure 10 shows the evolution of all 20 eigenvalues as a function of generation. The largest eigenvalues has an eigenvector dominated by the yield stress and the power law creep activation energy. The next largest eigenvalue has a corresponding eigenvector dominated by the surface diffusion activation energy. All

parameters are shown in Table II. The most significant parameters for each eigenvector are in bold down to the eigenvector dominated by the random variable.

Finally, the information gained from the GA optimization using the copper powder data can be used in terms of experimental design. Figure 11 shows the *a priori* average relative density for the unoptimized model distribution as a function of temperature and pressure where the simulation incorporates a 15000s ramp up and 15000s hold. Figure 12 shows the standard deviation of the average density of figure 11. Clearly the robustness of the model would benefit from sintering data collected within the vicinity of 1200K. After the model was optimized using hot pressing data (Wadley *et al*. 1991) an average expected densification plot can be generated. This is shown in figure 13. The uncertainty of figure 13 is shown in figure 14. From the comparison of figures 12 and 14 one can see how the maximum uncertainty of the model dropped from 0.164 to 0.053. This drop in maximum uncertainty along with the shifting in the uncertainty landscape indicates that the temperature and pressures regimes where the experimental data was collected were wisely chosen. If further experiments are to be conducted to ensure the robustness of the model, then sintering data in the vicinity of 1200K should be collected.

4.0 Conclusions

The application of Bayesian analysis to GA optimization of micromechanical powder densification models rectifies a number of deficiencies in the overall GA technique. First, the calculation of the PPD from the GA output allows for the suppression of the inherent stochasticity of the GA. Second, PCA of the resulting C_m provides not only a sensitivity analysis of the model parameters, but also a suitable stopping criteria for the optimization itself. Lastly, the generation of the PPD allows a distribution of optimal model parameter vectors to be applied to the physics of the forward problem. The distribution of the resulting outcomes are then used as a guide in experimental design.

5.0 Acknowledgments

Funded by the Department of Defense, the Department of Energy and Los Alamos National Laboratory which is operated by the University of California under contract number W-7405-ENG-36.

6.0 References

G. Antelman, 1997, “Elementary Bayesian Statistics,” Eds. A. Madansky, R. McCulloch, Edward Elgar Publishing, Inc., Lyme, NH.

T. Bayes, 1763, “An Essay towards solving a problem in the doctrine of Chances,” Philosophical Transactions of the Royal Society, 53, 370-418.

A. J. W. Duijndam, 1988a, “Bayesian Estimation in Seismic Inversion. Part I: Principles,” Geophysical Prospecting, 36, 878-898.

A. J. W. Duijndam, 1988b, “Bayesian Estimation in Seismic Inversion. Part II: Uncertainty Analysis,” Geophysical Prospecting, 36, 899-918.

P. Gerstoft and C. F. Mecklenbräuker, 1998, “Ocean Acoustic Inversion with Estimation of *a posteriori* probability distributions,” Journal of the Acoustical Society of America, 104, 2, 808-819.

S. Mallick, 1995, “Model-based Inversion of Amplitude-variations-with-offset Data Using a Genetic Algorithm,” Geophysics, 60, 4, 939-954.

B. J. Reardon, 1998a, “Fuzzy Logic Vs. Niched Pareto Multiobjective Genetic Algorithm Optimization,” Modeling and Simulation in Materials Science and Engineering, 6, 717-734, 1998, http://www.iop.org/Journals/ms

B. J. Reardon, 1998b, “Optimization of Densification Modeling Parameters of Beryllium Powder Using a Fuzzy Logic Based Multiobjective Genetic Algorithm,” Modeling and Simulation in Materials Science and Engineering, 6, 735-746, http://www.iop.org/Journals/ms

B. J. Reardon, 1998c, “Optimization of Densification Modeling Parameters of Copper Powder Using a Fuzzy Logic Based Multiobjective Genetic Algorithm,” LA-UR-98-0419, http://lib-www.lanl.gov/la-pubs/00412622.pdf

B. J. Reardon, 1999, “Model Inversion Using Bayesian Inference and Genetic Algorithms,” LA-UR-99-1980, Los Alamos National Laboratory, Los Alamos, NM 87545, April, http://lib-www.lanl.gov//la-pubs/00326698.pdf

D. Roberts, “The Warm Isopressing of Beryllium Powder,” in ‘Beryllium Science (U),’ JOWOG 22 / AVIS 522, Ed. J. E. Hanafee, UCRL-89338, Vol 2, p. 176, 1983.

M. K. Sen, B. B. Bhattacharya, P. L. Stoffa, 1993, “Nonlinear inversion of resistively sounding data,” Geophysics, 58, 4, 496-507.

M. K. Sen and P. L. Stoffa, 1992, “Rapid sampling of model space using genetic algorithms: Examples from seismic waveform inversion,” Geophysics Journal International, 108, 281-292.

M. K. Sen and P. L. Stoffa, 1996, “Bayesian inference, Gibb’s sampler and uncertainty estimation in geophysical inversion,” Geophysical Prospecting, 44, 313-350.

A. Tarantola, 1987, “Inverse Problem Theory, Methods for Data Fitting and Parameter Estimation,” Elsevier, Amsterdam.

H. N. G. Wadley, R. J. Schaefer, A. H. Kahn, M. F. Ashby, R. B. Clough, Y. Geffen, J. J. Wlassich, “Sensing and Modeling of the Hot Isostatic Pressing of Copper Pressing,” Acta Metallurgica Et Materialia, 39, 5, 979-986, 1991.

7.0 Tables

Table I. The final eigenvectors for the Beryllium powder optimization.

	ε_1	ε_2	ε_3	ε_4	ε_5	ε_6	ε_7
Sur. Eng.	0.00011248	6.3795e-06	-6.5527e-05	-3.5378e-07	-1.2178e-06	-0.0041734	0.0051256
Yield	9.2513e-07	1.3849e-08	-1.5460e-07	-1.8110e-10	-7.2969e-10	3.6466e-06	-9.5214e-07
Temp. Dep.	0.0034461	2.7925e-05	-0.00059309	5.8510e-07	9.0403e-08	-0.0022471	0.017168
PLC. Exp.	0.00090594	1.2912e-05	-0.00023453	1.0677e-09	-6.3828e-08	0.0052271	-0.0014506
PLC. Stress	3.6493e-07	7.7689e-09	-3.6120e-09	-1.4555e-10	-1.3043e-09	-1.7341e-05	1.9379e-05
PLC. Eng.	1.0035e-06	8.0725e-08	3.8145e-07	-5.7164e-10	7.0483e-09	1.5258e-05	-1.4037e-05
CreepTrans.	-5.8041e-06	-6.8814e-08	9.2116e-07	-8.3110e-10	-4.0534e-09	-3.1914e-05	9.9336e-06
PrexpCreep	0.010815	0.00018643	-0.0029950	5.4693e-06	-2.9666e-05	0.71296	-0.69432
VD pre-exp.	5.9044e-07	1.5409e-06	9.6264e-06	-4.9074e-05	1.0000	2.0417e-05	-2.0351e-05
VD Eng.	-9.8547e-06	-1.3947e-07	1.8058e-06	6.9023e-11	4.5048e-10	-1.2043e-05	-2.7372e-05
BD pre-exp.	1.2233e-05	-2.2073e-05	-2.7200e-05	1.0000	4.9223e-05	-1.4119e-05	-5.2395e-06
BD Eng.	-5.6123e-05	1.2140e-06	2.4132e-05	-2.3474e-08	5.5798e-08	-0.00015320	-0.00012594
SD pre-exp.	0.050752	-0.72637	0.68506	2.3168e-06	-5.4129e-06	0.016701	0.014173
SD Eng.	6.1806e-06	-4.3483e-08	-2.7242e-06	2.6070e-09	-2.8605e-09	1.1936e-05	1.9817e-05
BM pre-exp	-0.0073292	0.68594	0.72661	3.5670e-05	-8.1148e-06	0.028240	0.025171
BM Eng.	-8.8516e-05	-1.2388e-06	1.3237e-05	-3.1937e-09	5.4947e-09	-0.00017622	-0.00015877
Radius	-0.93644	-0.042811	0.012939	1.5561e-05	3.5423e-07	0.24936	0.24254
Stage 2	-0.33804	-0.0052319	0.046726	-4.7845e-06	1.0129e-06	-0.61387	-0.66917
Stage 1	0.077524	0.00039443	-0.019217	1.0468e-05	6.6762e-06	0.22648	0.10047
Random	0.0056966	6.5372e-05	-0.0010197	3.8898e-07	-4.3557e-08	0.015696	0.0079593

Table I. Continued.

	ε_8	ε_9	ε_{10}	ε_{11}	ε_{12}	ε_{13}	ε_{14}
Sur. Eng.	-0.0077778	0.057916	0.98378	-0.16828	-0.019973	0.0022180	9.7468e-05
Yield	-1.3695e-06	-0.00065307	0.00018013	-6.8174e-05	-0.00073525	0.0047875	-0.00093025
Temp. Dep.	-0.016621	0.99623	-0.047286	0.065238	0.021246	-0.0014269	0.00022052
PLC. Exp.	-0.011096	-0.020708	0.022208	0.0042630	**0.99937**	-0.012292	3.1544e-05
PLC. Stress	5.5513e-07	3.2484e-05	-3.3308e-05	-6.6479e-05	-0.00034518	-0.0073374	0.0060186
PLC. Eng.	6.8684e-05	0.00011073	8.6153e-05	-0.00016873	0.0016713	0.014948	-0.00055156
CreepTrans.	1.2135e-06	-0.00012776	-0.00016024	-3.7454e-05	0.0027119	-0.0087860	0.015513
PrexpCreep	0.095800	0.015330	0.0069697	0.0031952	-0.0035318	0.00021930	-1.1731e-05
VD pre-exp.	9.5095e-06	6.5311e-07	1.3229e-06	-3.0670e-07	2.2015e-08	7.6917e-08	5.0895e-09
VD Eng.	4.8562e-05	-8.4873e-05	-6.5184e-05	1.1946e-06	-0.00016319	-0.0078271	-0.013486
BD pre-exp.	8.5119e-06	-4.1694e-07	4.1154e-07	-6.7545e-08	2.5589e-07	4.2805e-09	5.3993e-10
BD Eng.	0.0020476	-0.0011263	0.0023570	0.0015630	-0.012363	**-0.99881**	0.023951
SD pre-exp.	-0.0044667	-2.9158e-05	1.1177e-05	1.8010e-05	6.8565e-06	-7.3459e-07	-1.1131e-07
SD Eng.	-0.00024070	-0.00010371	-1.8237e-05	-1.3234e-05	-3.2897e-05	-0.032452	0.080004
BM pre-exp	-0.0055290	-2.5823e-05	-3.1699e-06	3.3093e-05	-4.8601e-06	8.8834e-08	-3.8337e-08
BM Eng.	7.5369e-05	0.00028144	-0.00012846	-0.0015070	-0.00020763	-0.026709	**-0.99628**
Radius	0.0082837	-0.00024785	3.1416e-05	0.00028797	-1.4760e-05	2.0898e-06	7.0509e-07
Stage 2	-0.24231	0.0078331	-0.0032491	-0.010522	0.00014197	-0.00032387	0.00024927
Stage 1	-0.96488	-0.019168	-0.0017546	0.026681	-0.012321	-0.0018110	-0.00015363
Random	-0.023096	0.055546	-0.17142	**-0.98314**	0.0087948	-0.0021214	0.0015544

Table I. Continued.

	ε_{15}	ε_{16}	ε_{17}	ε_{18}	ε_{19}	ε_{20}
Sur. Eng.	8.0638e-05	-2.5115e-06	-0.00011142	0.00025125	0.00016984	-5.0269e-05
Yield	-0.0035770	-0.021474	-0.032377	-0.017202	**-0.98930**	**0.13945**
Temp. Dep.	3.0459e-05	-7.2930e-05	-1.1258e-05	0.00011664	-0.00067506	0.00013318
PLC. Exp.	-0.00037367	-0.00094490	0.0029905	-0.00049684	-0.00085793	-4.0887e-05
PLC. Stress	-0.019574	0.023571	0.042594	0.036240	**-0.14175**	**-0.98780**
PLC. Eng.	-0.015363	-0.021993	**-0.62746**	**-0.77531**	0.026220	-0.059598
CreepTrans.	0.0025469	**0.32893**	**-0.73835**	**0.58845**	0.0062744	-0.0031917
PrexpCreep	3.8902e-05	2.4816e-05	-1.3197e-05	4.4859e-05	-6.6994e-06	-2.4620e-05
VD pre-exp.	7.6895e-09	2.0447e-09	1.8835e-09	1.0918e-08	-1.0092e-09	-2.1001e-09
VD Eng.	-0.066821	**-0.94122**	**-0.24015**	**0.22496**	0.020893	-0.026260
BD pre-exp.	4.6947e-10	-4.4425e-10	-3.7208e-11	5.0252e-11	4.7073e-15	4.0531e-17
BD Eng.	-0.034016	0.0056524	-0.00053573	-0.019092	-0.0033493	0.0081353
SD pre-exp.	-1.0885e-07	5.3368e-08	-1.4896e-09	1.0860e-08	4.6489e-11	6.5851e-13
SD Eng.	**0.99366**	-0.064938	-0.022495	0.0011156	-0.0046273	-0.020777
BM pre-exp	-7.0243e-08	2.5547e-08	3.0917e-09	-1.3052e-08	-4.3026e-10	-8.4455e-12
BM Eng.	0.079814	0.012958	-0.0094302	0.0064128	-0.00058456	-0.0072316
Radius	-9.3611e-09	2.9800e-08	-1.1692e-07	6.1443e-08	-1.4157e-07	-5.1836e-09
Stage 2	-6.4686e-05	1.1467e-05	8.7124e-06	-3.1777e-05	-7.8670e-06	4.2642e-06
Stage 1	-0.00029013	-6.8582e-06	-9.4992e-05	-6.9998e-05	1.9912e-05	7.9151e-06
Random	-0.00020623	-2.8732e-05	0.00017736	3.0633e-05	-7.8936e-06	0.00010910

Table II. The final eigenvectors for the Copper powder optimization.

	ε_1	ε_2	ε_3	ε_4	ε_5	ε_6	ε_7
Sur. Eng.	-0.00084031	-6.1180e-05	2.7414e-07	6.9684e-06	5.4140e-05	0.00029394	0.0041409
Yield	5.8670e-06	4.6447e-07	4.1442e-09	1.2387e-08	-2.4983e-07	-4.9154e-06	-2.3794e-05
Temp. Dep.	-0.00079738	-2.1943e-05	1.4217e-06	5.8068e-05	5.1199e-06	-0.00086217	0.0041114
PLC. Exp.	-0.00013277	-8.0210e-05	-7.4596e-07	2.4906e-05	2.2214e-05	0.0017448	-0.0010393
PLC. Stress	5.2389e-06	-3.3131e-07	-9.2456e-09	-1.3849e-07	2.1703e-07	2.4794e-05	-4.3468e-05
PLC. Eng.	-9.8586e-06	-2.0938e-06	-1.5411e-08	2.8659e-07	3.5657e-07	4.2125e-05	-1.6416e-06
CreepTrans.	7.6916e-05	1.6145e-05	3.3817e-08	-2.1675e-06	-1.9154e-06	-0.00032948	3.4796e-05
PrexpCreep	-0.010270	0.00082649	-4.1144e-06	-0.00081499	0.0010398	-0.021601	0.093780
VD pre-exp.	3.7619e-06	-6.6044e-05	1.00000	-0.0026832	-3.5957e-05	1.1085e-05	-8.9027e-07
VD Eng.	-3.5544e-06	7.0759e-07	-2.1839e-08	-3.2696e-07	3.2003e-07	-2.1966e-05	4.7236e-05
BD pre-exp.	-0.00059443	0.043710	-0.0026778	-0.99902	-0.0061716	0.0031623	-0.00035279
BD Eng.	-9.9346e-05	-7.4245e-06	2.8855e-08	6.8400e-07	2.7844e-06	5.7276e-05	0.00039726
SD pre-exp.	-0.013063	0.81452	0.00016060	0.032154	0.57851	0.025917	0.0015074
SD Eng.	-3.5115e-06	2.5714e-08	-3.5525e-09	-3.1401e-08	9.2185e-08	-6.0904e-06	2.3851e-05
BM pre-exp	0.032267	0.57655	8.9765e-05	0.030363	-0.81462	0.041207	0.018224
BM Eng.	6.8267e-06	9.7983e-07	-1.8271e-09	-2.5863e-08	-2.8152e-07	-1.9956e-05	-1.1046e-05
Radius	-0.95596	0.019590	8.5233e-06	0.0010590	-0.039152	-0.21330	-0.19676
Stage 2	0.19671	0.0089860	7.8492e-08	0.00066049	-0.0065390	0.022138	-0.97555
Stage 1	-0.21479	-0.042048	-8.9680e-06	0.0013007	0.010674	0.97527	-0.019607
Random	-0.0010244	-3.1621e-05	4.0833e-07	2.5461e-05	-9.9781e-07	-0.0015052	0.0058367

Table II. Continued.

	ε_8	ε_9	ε_{10}	ε_{11}	ε_{12}	ε_{13}	ε_{14}
Sur. Eng.	-0.015227	-0.010732	-0.10612	**0.98832**	-0.10764	0.0015712	2.8521e-05
Yield	3.1159e-05	0.00012930	-9.3557e-05	0.00018965	0.00082817	-0.0065512	-0.018256
Temp. Dep.	0.038729	0.98758	-0.10948	0.010995	**0.10508**	-0.00058959	-0.0041054
PLC. Exp.	-0.012871	0.096757	-0.088632	**-0.11589**	**-0.98444**	0.00086065	0.0067974
PLC. Stress	-0.00042803	4.6017e-05	-0.0014597	-0.00071073	-0.0036236	-0.025005	**-0.24600**
PLC. Eng.	0.00019980	-0.00078858	-0.0010115	0.00064983	-0.0024100	0.025787	0.17626
CreepTrans.	-0.0023403	0.0031388	-0.0031553	0.00060210	0.0066839	**-0.32534**	**0.89931**
PrexpCreep	-0.99349	0.031672	-0.042652	-0.017556	0.021854	-0.00021476	-0.0025971
VD pre-exp.	-2.4978e-06	-1.0815e-06	3.0019e-07	-2.9867e-07	-8.2417e-07	3.8496e-08	-2.0396e-08
VD Eng.	-0.00031172	0.00028159	-0.00020253	-0.00056099	0.00028035	-0.039329	**-0.11072**
BD pre-exp.	0.00075410	3.5878e-05	-9.6652e-06	1.7729e-05	-3.0482e-05	-8.8641e-08	8.2510e-09
BD Eng.	0.0010296	-0.0016439	0.0012375	0.0014111	-0.0034598	**-0.94364**	-0.29327
SD pre-exp.	0.00096951	-1.6862e-05	-1.4132e-06	5.6525e-06	-2.1318e-05	1.3116e-07	-1.5507e-08
SD Eng.	5.2450e-06	0.00024274	4.1585e-05	0.00040328	-0.00028880	-0.024824	-0.030374
BM pre-exp	9.2355e-05	-1.0507e-06	-4.6758e-06	1.7806e-05	-1.8103e-05	9.8438e-08	-3.7556e-08
BM Eng.	-1.7720e-05	-0.00010625	-0.00074828	0.00023010	0.00013567	0.013964	-0.0071669
Radius	-0.0040775	1.7247e-05	-2.5444e-05	1.4277e-05	1.1771e-05	9.2741e-08	3.1246e-08
Stage 2	-0.093895	0.0063203	-0.010752	0.0021101	0.0036073	-0.00041547	-0.00037976
Stage 1	-0.020670	0.0010830	-0.0021309	-0.00066454	0.0024306	-5.4071e-05	0.00024727
Random	0.042665	-0.11897	-0.98333	-0.096703	0.087638	-0.00030354	-0.0030846

Table II. Continued.

	ε_{15}	ε_{16}	ε_{17}	ε_{18}	ε_{19}	ε_{20}
Sur. Eng.	0.00094864	-0.00061828	-0.00054108	0.00045964	0.00034669	-6.1280e-06
Yield	-0.024042	**0.13418**	-0.021218	-0.015275	0.034436	**0.98953**
Temp. Dep.	-0.0018157	0.00053291	0.00082655	-0.00016776	0.00040478	-0.00042554
PLC. Exp.	0.0013451	-0.0037974	-0.00010114	0.00045052	-6.6869e-06	0.0015092
PLC. Stress	**0.59475**	**0.72026**	**-0.22206**	-0.090462	-0.00036184	-0.094061
PLC. Eng.	**-0.74583**	**0.61850**	**-0.11584**	-0.074634	0.0027856	**-0.10229**
CreepTrans.	**0.25723**	0.045382	**-0.12713**	-0.0043702	-0.027454	0.012690
PrexpCreep	-0.0012386	-0.00019589	0.00084224	-3.3003e-06	0.00012647	-2.8855e-05
VD pre-exp.	-1.3477e-08	5.3874e-09	-2.0557e-08	2.7255e-10	-4.2356e-09	-4.7398e-09
VD Eng.	-0.091935	**-0.23405**	**-0.94670**	**0.15677**	-0.044967	0.010885
BD pre-exp.	-1.2849e-08	1.4005e-10	1.2041e-10	-5.2050e-12	1.9003e-12	-6.4592e-15
BD Eng.	**-0.12073**	-0.011822	0.082958	-0.019879	0.036807	-0.012795
SD pre-exp.	2.1600e-08	3.6343e-09	3.8883e-09	-3.9747e-10	3.5898e-10	-5.8171e-12
SD Eng.	-0.010068	0.021118	0.053192	0.031071	**-0.99653**	0.032467
BM pre-exp	1.8071e-08	2.8653e-08	1.2816e-08	1.2631e-08	-4.7538e-08	4.8390e-09
BM Eng.	-0.011451	**-0.15245**	-0.12124	**-0.97982**	-0.040135	0.0040247
Radius	-6.5950e-08	4.7576e-08	1.4462e-07	-6.1678e-08	-4.9491e-08	-3.1668e-08
Stage 2	-0.00020113	-7.1256e-05	8.6852e-05	2.1457e-05	2.9778e-06	-2.9784e-05
Stage 1	7.9806e-05	-3.4072e-05	-4.1006e-05	-1.1500e-05	-1.6368e-05	1.4375e-05
Random	-0.0010292	-0.0013545	0.0011907	0.00084453	3.9067e-05	3.4774e-06

8.0 Figures

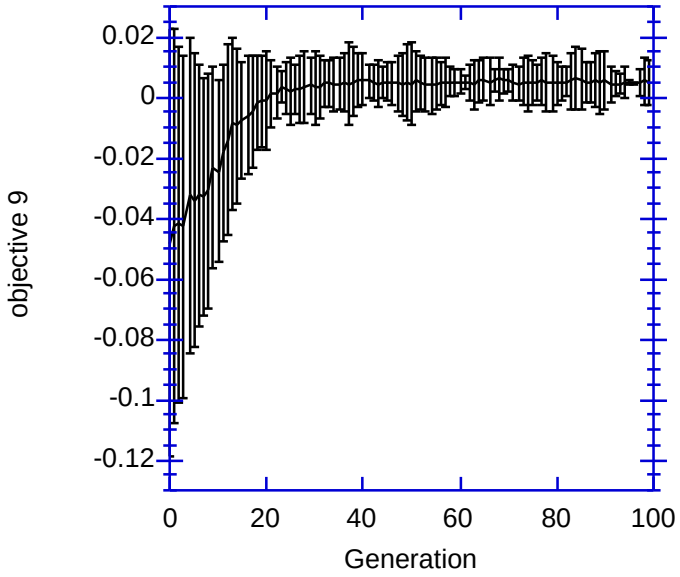

Figure 1. The average objective value for the entire population as a function of generation along with the standard deviation of the average (Reardon 1998b).

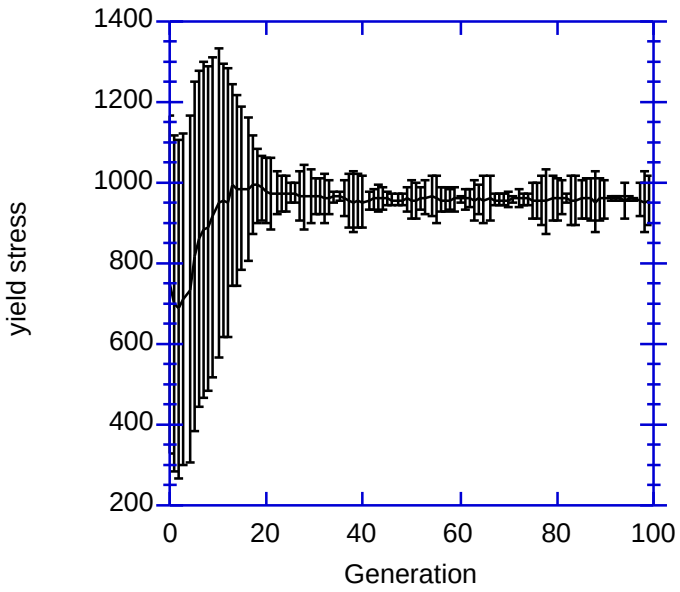

Figure 2a. The average value for the beryllium yield stress as a function of generation along with the standard deviation (Reardon 1998b).

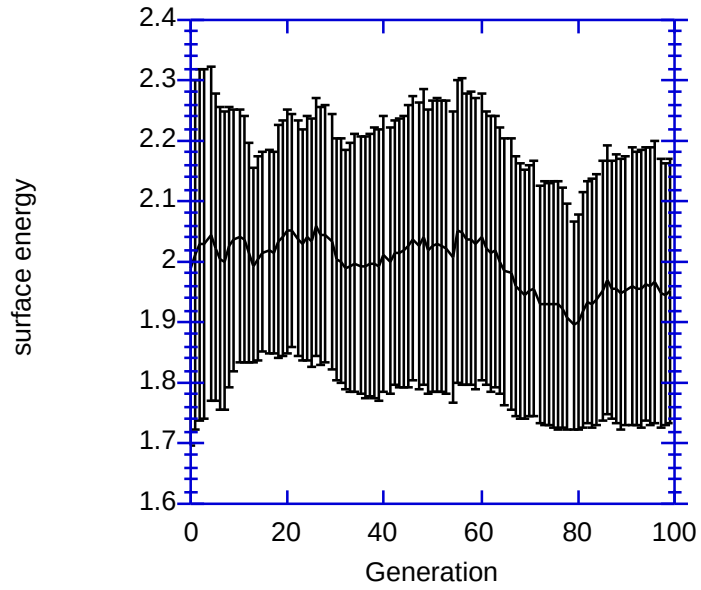

Figure 2b. The average value for the beryllium surface energy as a function of generation along with the standard deviation (Reardon 1998b).

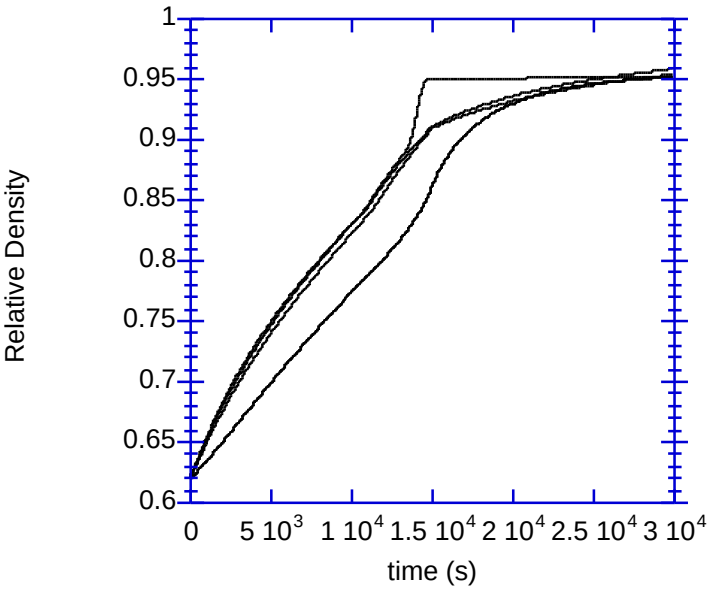

Figure 3. Five GA optimized copper powder densification models (Reardon 1998c). All of the models reach the same final end point but the path each took to get there is considerably different.

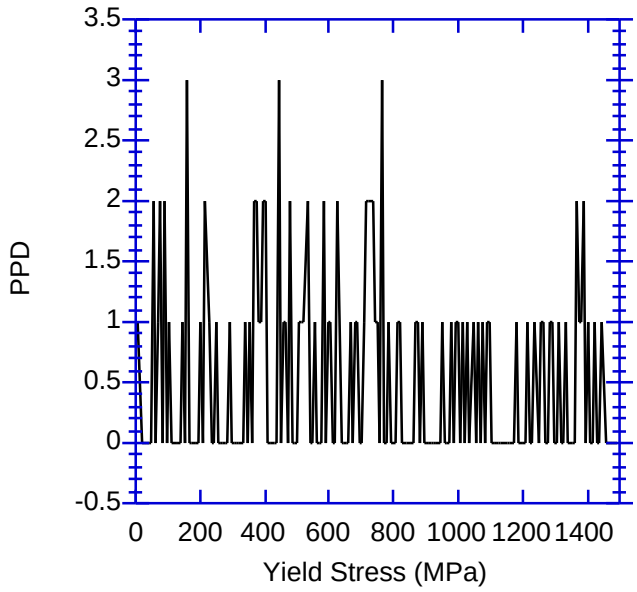

Figure 4a. The unnormalized beryllium yield stress marginal PPD at generation 0.

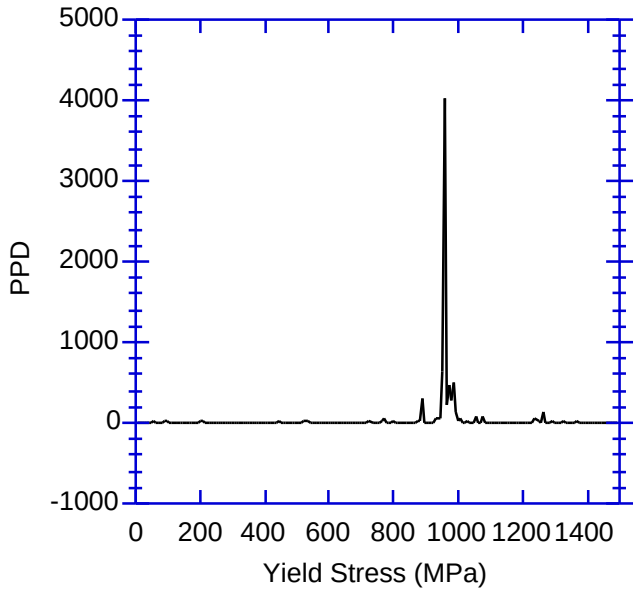

Figure 4b. The unnormalized beryllium yield stress marginal PPD at generation 80.

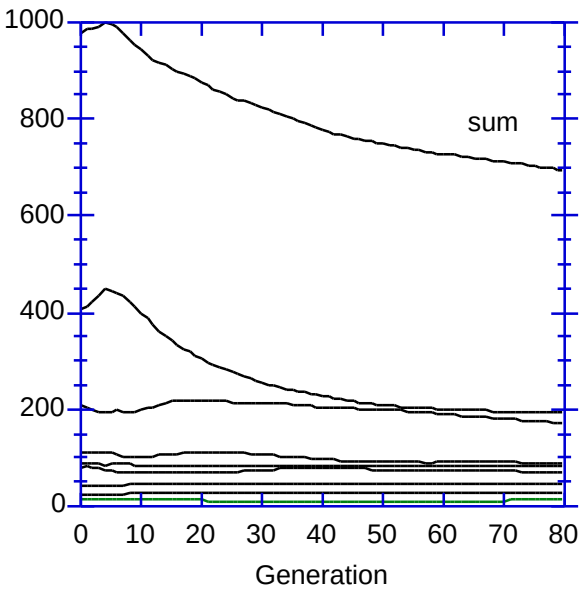

Figure 5. The evolution of all 20 eigenvalues from the Beryllium powder optimization as a function of generation.

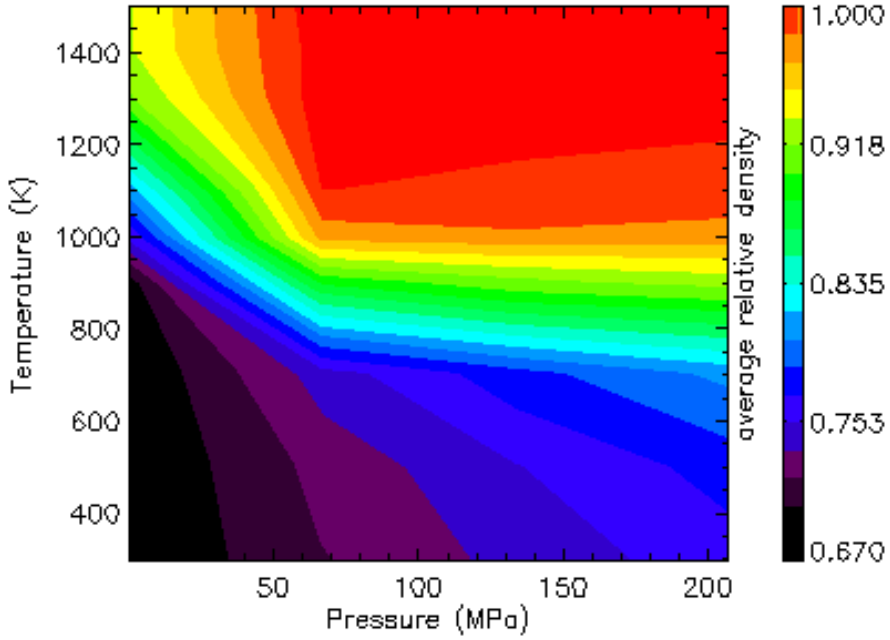

Figure 6. The *a priori* average model density for beryllium powder as a function of temperature and pressure assuming a 1 hour ramp up, hold and ramp down.

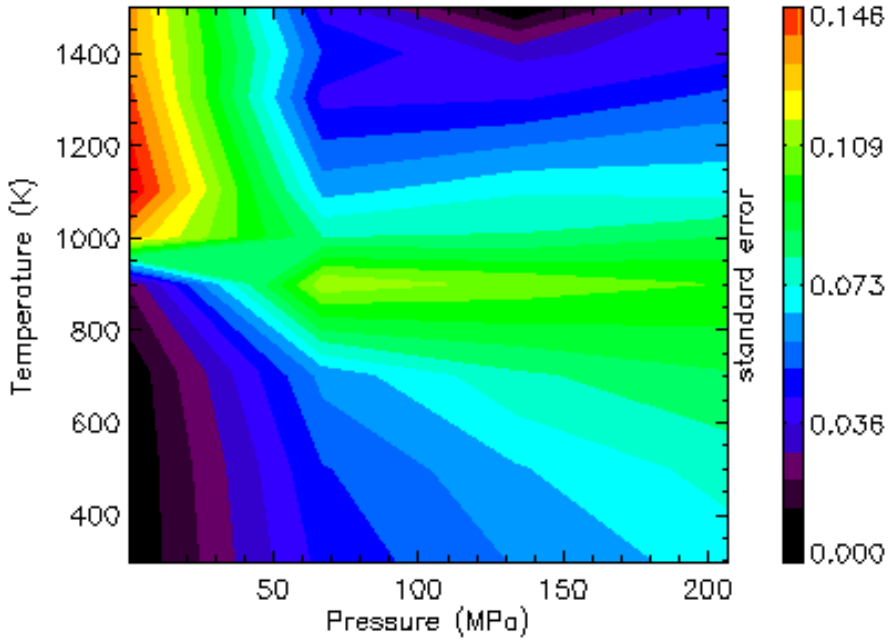

Figure 7. The standard deviation in the *a priori* average model density of figure 6.

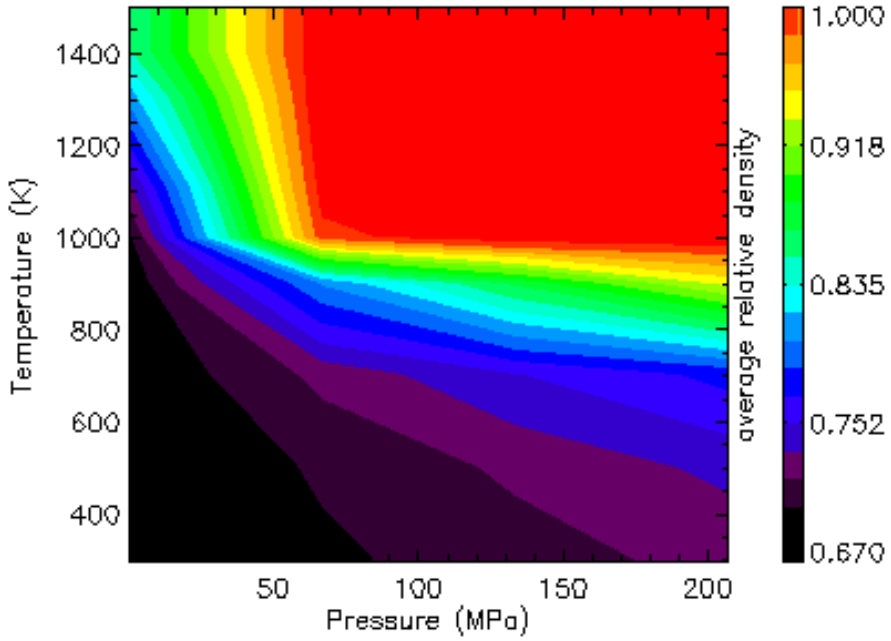

Figure 8. The *a posteriori* average model density for beryllium powder as a function of temperature and pressure assuming a 1 hour ramp up, hold and ramp down.

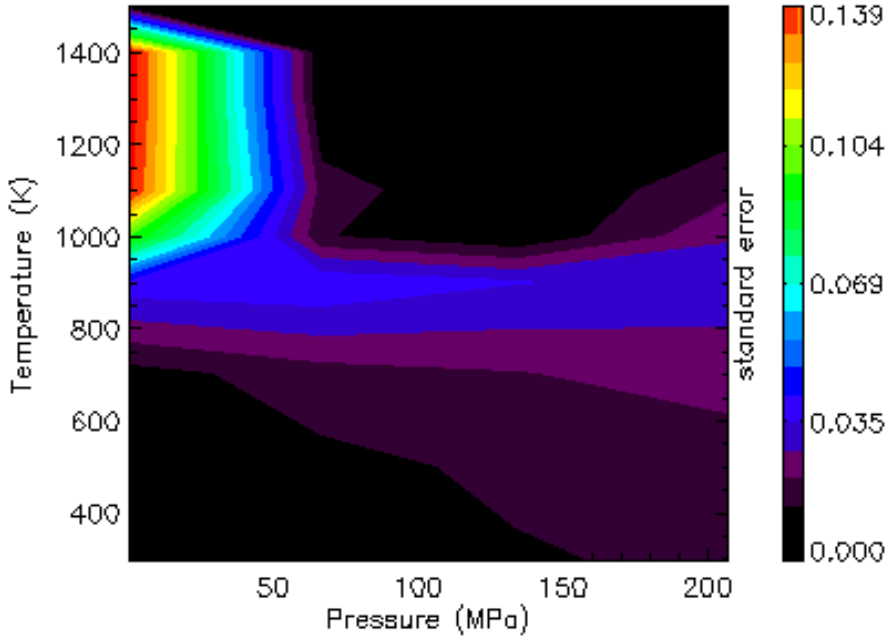

Figure 9. The standard deviation in the *a posteriori* average model density of figure 8.

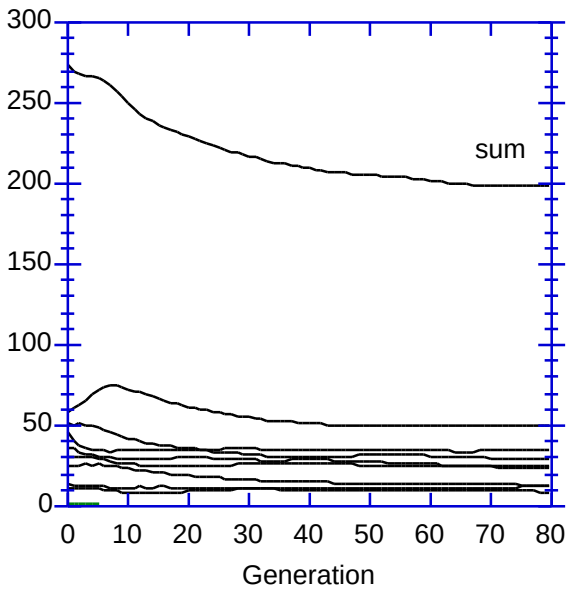

Figure 10. The evolution of all 20 eigenvalues from the copper powder optimization as a function of generation.

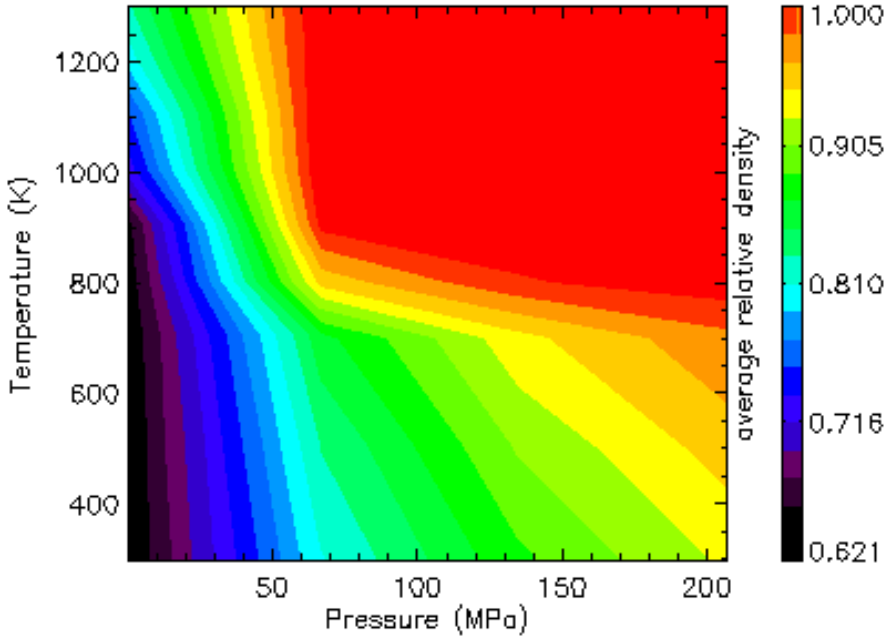

Figure 11. The *a priori* average model density for copper powder as a function of temperature and pressure assuming a 15000s ramp up and a 15000s hold.

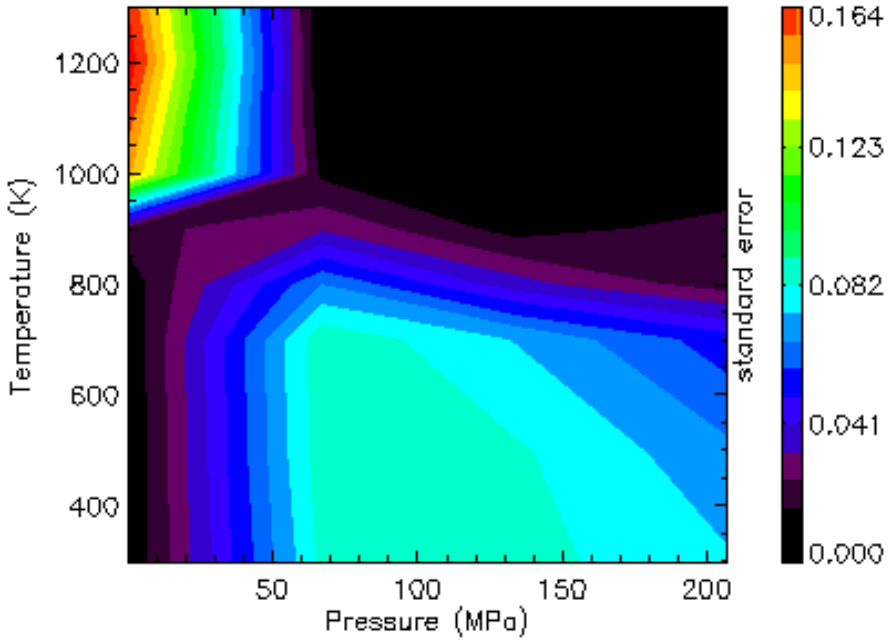

Figure 12. The standard deviation in the *a priori* average model density of figure 11.

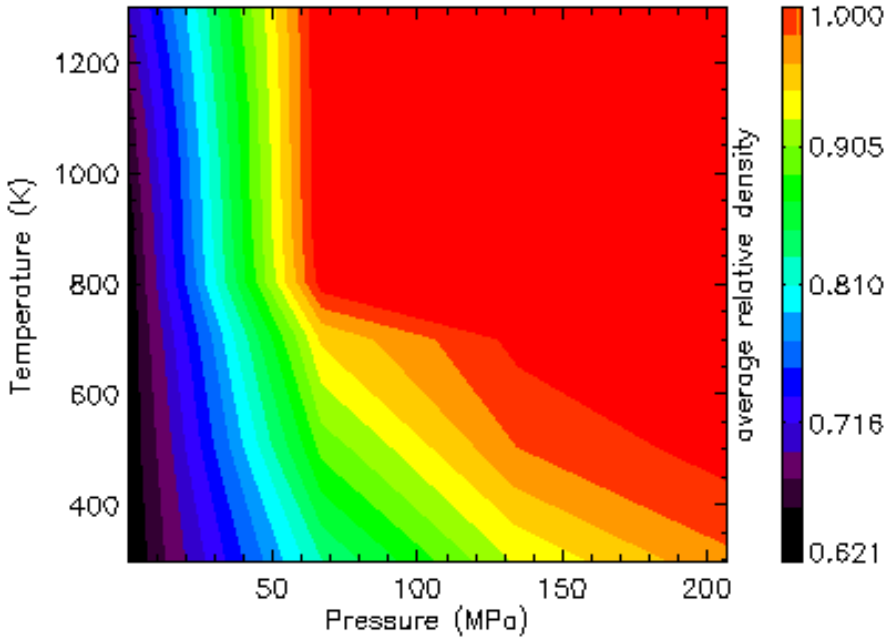

Figure 13. The *a posteriori* average model density for copper powder as a function of temperature and pressure assuming a 15000s ramp up and 15000s hold.

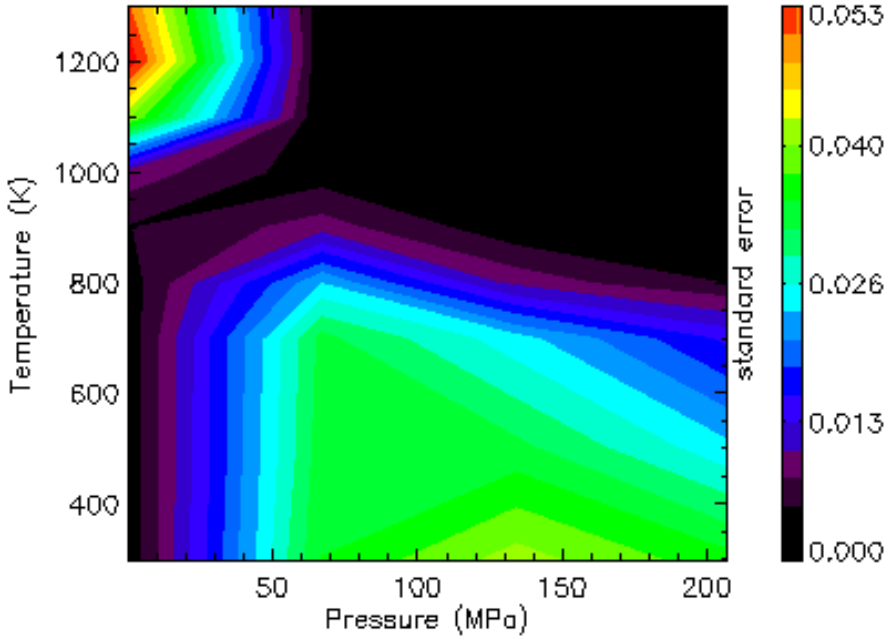

Figure 14. The standard deviation in the *a posteriori* average model density of figure 13.